ELSEVIER
爱思唯尔

国际医学名著精品系列 （英文原版）

Body MRI

体部磁共振成像

Evan S. Siegelman

人民軍醫出版社
PEOPLE'S MILITARY MEDICAL PRESS

国际医学名著精品系列 （英文原版）

Body MRI

体部磁共振成像

Evan S. Siegelman, MD

Associate Professor of Radiology
Chief, MRI Section
Department of Radiology
Hospital of the University of Pennsylvania
Philadelphia, PA

ELSEVIER
爱思唯尔

人民軍醫出版社
PEOPLE'S MILITARY MEDICAL PRESS

北 京

图书在版编目（CIP）数据

体部磁共振成像＝Body MRI：英文/（美）西格尔曼（Siegelman，E．S.）编著．-北京：人民军医出版社，2007.4
ISBN 978-7-5091-0788-1

Ⅰ.体... Ⅱ. 西... Ⅲ.磁共振成像-英文 Ⅳ.R445.2

中国版本图书馆 CIP 数据核字（2007）第 042959 号

著作权合同登记号：图字-军-2007-010

策划编辑：高爱英
出 版 人：齐学进
出版发行：人民军医出版社　　**经　销**：新华书店
通信地址：北京市 100036 信箱 188 分箱　**邮　编**：100036
电话：（010）66882586（发行部）、51927290（总编室）
传真：（010）68222916（发行部）、66882583（办公室）
网址：www.pmmp.com.cn

印装：北京佳信达艺术印刷有限公司
开本：889 mm×1 194 mm　1/16
印张：33.75　**字数**：1 496 千字
版、印次：2007 年 4 月第 1 版第 1 次印刷
印数：0001～1 500
定价：178.00 元

Body MRI, 1st edition
Evan S. Siegelman
ISBN-13: 9780721637402
ISBN-10: 072163740X

Authorized reprint edition from English edition published by the Proprietor.
ISBN-13: 9789812599636
ISBN-10: 9812599630

Elsevier (Singapore) Pte Ltd.
3 Killiney Road
#08-01 Winsland House I
Singapore 239519
Tel: (65) 6349-0200
Fax: (65) 6733-1817

First Published 2007
2007 年初版

Printed in China by People's Military Medical Press under special arrangement with Elsevier (Singapore) Pte Ltd. This edition is authorized for sale in China only, excluding Hong Kong SAR and Taiwan. Unauthorized export of this edition is a violation of the Copyright Act. Violation of this Law is subject to Civil and Criminal Penalties.

本书英文影印版由 Elsevier (Singapore) Pte Ltd. 授权人民军医出版社在中国大陆境内独家发行。本版仅限在中国境内（不包括香港特别行政区及台湾）出版及标价销售。未经许可之出口，视为违反著作权法，将受法律之制裁。

I dedicate this book to my father, Stanley S. Siegelman, MD, and to the memory of my mother, Doris F. Siegelman.

Contributors

Saroja Adusumilli, MD
Assistant Professor of Radiology, Department of Radiology, University of Michigan Health System, Ann Arbor, MI

Laura Carucci, MD
Assistant Professor, Director of MR Imaging, Director of Abdominal MR, Department of Radiology, Virginia Commonwealth University Medical Center, Richmond, VA

Adam Fisher, MD
Staff Radiologist, Department of Radiology, Crozer Chester Medical Center, Upland, PA

Anne M. Hubbard, MD
Associate Professor of Radiology, University of Pennsylvania Medical School; Staff Radiologist, Department of Radiology, Children's Hospital of Philadelphia, Philadelphia, PA

E. Scott Pretorius, MD
Wallace T. Miller Sr. Chair of Radiologic Education, Residency Program Training Director, Department of Radiology, Hospital of the University of Pennsylvania, Philadelphia, PA

David Roberts, MD, PhD
Director of CT/MRI, Department of Radiology, Kennedy Health System, Voorhees, NJ

Mark A. Rosen, MD, PhD
Assistant Professor of Radiology, Department of Radiology, Hospital of the University of Pennsylvania, Philadelphia, PA

Evan S. Siegelman, MD
Associate Professor of Radiology, Chief, MRI Section, Department of Radiology, Hospital of the University of Pennsylvania, Philadelphia, PA

Drew A. Torigian, MD, MA
Assistant Professor of Radiology, Department of Radiology, Hospital of the University of Pennsylvania, Philadelphia, PA

Preface

MR is a powerful imaging tool in the evaluation of disease processes of the thorax, abdomen, and pelvis, but some radiologists are uncomfortable performing and interpreting body MR examinations. This book is an attempt to familiarize the target audience (radiology residents, fellows, and practicing radiologists trained before the maturation of body MR) with the MR findings of normal anatomy and common entities encountered in clinical practice. It is my hope that the reader will use this text to assist him or her in establishing specific MR tissue diagnoses (the "elusive tissue signature"[1]) and to accurately diagnose and stage neoplasms.

I have modeled the format of this textbook on the highly successful *Musculoskeletal MRI*.[2] Specific MR techniques and physical principles are addressed in individual chapters where appropriate. Some topics, such as MR techniques and physics, are not covered in this textbook. For those who desire supplementary material, dedicated textbooks and reviews are available.[3-5] Reviews of MR imaging of the small and large bowel are also available elsewhere.[6-8] MR techniques used to evaluate cardiac structure and function, myocardial viability and perfusion,[9-13] and the coronary arteries[14,15] are still evolving.[16] Those interested in additional reading can consult available texts[17,18] or a recent issue of the *MR Clinics of North America* devoted to this "hot topic."[19] Body applications of functional MR techniques have not been widely incorporated into clinical practice. I anticipate that we shall adopt functional techniques to evaluate tumor viability and to differentiate between reactive and malignant lymph nodes.[20,21]

I thank my friends-colleagues at the University of Pennsylvania Health System for their efforts in the preparation of this text. I would also like to acknowledge the patience and support of my wife, Debby Michelman, and our three sons, Daniel, Matthew, and Dylan.

Respectfully,

Evan S. Siegelman, MD

REFERENCES

1. Rogers LF. Imaging: a Sisyphean search for the elusive tissue signature. AJR Am J Roentgenol 2002;179(3):557.
2. Kaplan P, A., Helms CA, Dussault R, Anderson MW, Major NM, editors. Musculoskeletal MRI, 1st ed. Philadelphia, W. B. Saunders, 2001.
3. Horowitz AL. MR physics for radiologists: A visual approach. 3rd ed. New York, Springer, 1994.
4. Mitchell DG, Cohen, MS. MRI Principles. 2nd ed. Philadelphia, W. B. Saunders 2004.
5. Constable RT. MR physics of body MR imaging. Radiol Clin North Am 2003;41(1):1-15, v.
6. Lomas DJ. Techniques for magnetic resonance imaging of the bowel. Top Magn Reson Imaging 2002;13(6):379-387.
7. Umschaden HW, Gasser J. MR enteroclysis. Radiol Clin North Am 2003;41(2):231-248.
8. Lauenstein TC. Magnetic resonance imaging in bowel imaging. Top Magn Reson Imaging 2002;13(6):377.
9. Kim RJ, Wu E, Rafael A, Chen EL, Parker MA, Simonetti O, et al. The use of contrast-enhanced magnetic resonance imaging to identify reversible myocardial dysfunction. N Engl J Med 2000;343(20):1445-1453.
10. Earls JP, Ho VB, Foo TK, Castillo E, Flamm SD. Cardiac MRI: Recent progress and continued challenges. J Magn Reson Imaging 2002;16(2):111-127.
11. Duerinckx AJ. Myocardial viability using MR imaging: is it ready for clinical use? AJR Am J Roentgenol 2000;174(6): 1741-1743.
12. Wagner A, Mahrholdt H, Holly TA, et al. Contrast-enhanced MRI and routine single photon emission computed tomography (SPECT) perfusion imaging for detection of subendocardial myocardial infarcts: an imaging study. Lancet 2003;361(9355):374-379.
13. Castillo E, Bluemke DA. Cardiac MR imaging. Radiol Clin North Am 2003;41(1):17-28.
14. Kim WY, Danias PG, Stuber M, Flamm SD, Plein S, Nagel E, et al. Coronary magnetic resonance angiography for the detection of coronary stenoses. N Engl J Med 2001;345(26): 1863-1869.
15. Achenbach S, Daniel WG. Noninvasive coronary angiography—an acceptable alternative? N Engl J Med 2001; 345(26):1909-1910.
16. Polak JF. MR coronary angiography: are we there yet? Radiology 2000;214(3):649-650.
17. Duerinckx AJ, editor. Coronary Magnetic Resonance Angiography. New York, Springer-Verlag, 2002.
18. Manning WJ, Pennell DJ. Cardiovascular Magnetic Resonance. Philadelphia, Churchill Livingstone, 2002.
19. Woodward P. Cardiac MR imaging. MR Clinics of North America 2003;11(1):1-191.
20. Choyke PL, Dwyer AJ, Knopp MV. Functional tumor imaging with dynamic contrast-enhanced magnetic resonance imaging. J Magn Reson Imaging 2003;17(5):509-520.
21. Koh DM, Cook GJ, Husband JE. New horizons in oncologic imaging. N Engl J Med 2003;348(25):2487-2488.

Protons dance and sing
Reveal our inner secrets
To the naked eye

Contents

1

Body MR Techniques and MR of the Liver

Adam Fisher, MD
Evan S. Siegelman, MD

Magnetic resonance (MR) imaging provides comprehensive evaluation of the liver including the parenchyma, biliary system, and vasculature. While computed tomography and sonography are often the initial studies used in evaluating the liver, MR is increasingly relied upon as a primary imaging modality in addition to its problem-solving capacity. MR provides soft tissue characterization unachievable with other imaging modalities. Lack of ionizing radiation and relative lack of operator dependence are additional advantages over computed tomography and ultrasound, respectively. Rapid breath-hold pulse sequences have largely supplanted older, slower pulse sequences, resulting in shortened examination times. After a brief review of current techniques, this chapter will focus on MR imaging manifestations of liver diseases, with an emphasis on pathologic correlation.

FIELD STRENGTH AND SURFACE COILS

Ideally, MR imaging of the liver is performed on high-field systems greater than 1.0 tesla (T), with open, low-field systems reserved for claustrophobic or obese patients. Phased-array surface coils provide improved signal-to-noise and contrast-to noise ratios, and better lesion detection and conspicuity in comparison with the conventional body coil surrounding the bore of the scanner.[1] Proximity of anterior abdominal wall subcutaneous fat to the surface coil can result in respiratory motion artifact "ghosts" projecting over the image. This artifact can be eliminated or minimized with breath-holding sequences or fat suppression.[1]

MR PULSE SEQUENCES

T1-Weighted Imaging (T1-WI)

The liver has a T1-relaxation time shorter than that of other abdominal tissues except for fat and pancreas. This short T1-relaxation time of liver has been attributed to abundant rough endoplasmic reticulum and high rate of protein synthetic activity (Box 1-1).[2] Hepatic lesions that are isointense or hyperintense to liver parenchyma on T1-weighted images (T1-WIs)

1-1 Causes of High Signal Intensity (SI) on Unenhanced T1-WI

- Protein (common; cause of normal high SI of hepatocytes)
- Lipid (common)
- Hemorrhage
- Paramagnetic substances (e.g., melanin, gadolinium)
- Blood flow

are usually of hepatocellular origin (Box 1-2). Lesions of other cellular origin such as cysts, hemangiomas, and metastases typically have a longer T1-relaxation time than does liver and will appear hypointense to liver parenchyma on T1-WIs.

Breath-hold gradient-echo (GRE) pulse sequences can replace spin-echo (SE) images for T1-WI of the liver. T1-W GRE sequences can be performed with multishot or single-shot techniques.[3] The term shot refers to the number of excitation pulses used in a pulse sequence. Multishot spoiled GRE T1-W sequences utilize a short repetition time (TR), short echo time (TE), and a high flip angle of 70° to 90°.[3] The lack of 180° refocusing pulses in GRE sequences allow water and lipid protons to precess in and out of phase with varying echo times. At 1.5 T, water and lipid are in phase at a TE range of 4.2 to 4.6 ms and out of phase at a TE range of 2.1 to 2.3 ms. Dual GRE T1-W sequences enable simultaneous acquisition of in-phase and opposed-phase images with two echo times per excitation. On in-phase images, signal from water and lipid within the same voxel are additive, whereas on opposed phase images, destructive interference of water and lipid protons results in loss of signal intensity (SI).

The combination of in-phase and opposed-phase images, referred to as chemical shift imaging, allows detection of hepatic steatosis as well as intralesional lipid in hepatocellular neoplasms such as hepatic adenoma and well-differentiated hepatocellular carcinoma (Box 1-3). Chemical shift refers to the difference in resonant frequency between two types of protons, with the resonant frequency of a proton dependent on its local molecular environment. Chemical shift imaging is optimal for detection of microscopic lipid, whereas chemically selective fat-suppression techniques are best for the macroscopic lipid present in subcutaneous and intraabdominal fat or macroscopic fat containing tumors such as adrenal myelolipoma (see Chapter 3), renal angiomyolipoma (see Chapter 4), and ovarian dermoid cysts (see Chapter 7).

In patients with limited breath-holding capacity, rapid T1-WIs can be obtained with magnetization-prepared GRE pulse sequences.[3] A single section can be obtained in less than 1.5 sec with negligible effects from respiratory motion. This sequence incorporates a section-selective 180° inversion pulse and produces T1-WIs with high SI blood vessels; most lesions will appear hypointense on this sequence. The inversion pulse and inversion time can also be manipulated to produce T1-WIs with low SI blood vessels, a feature that minimizes pulsation artifacts.

1-2 Isointense-hyperintense Liver Lesions on Unenhanced T1-WI

Hepatocellular (Common)

Focal nodular hyperplasia
Hepatic adenoma
Focal hepatic steatosis (in-phase imaging)
Focal sparing of steatosis (opposed-phase imaging)
Regenerative nodule
Hepatocellular carcinoma

Nonhepatocellular (Uncommon)

Hematoma (methemoglobin within rim)
Hemorrhagic metastases (e.g., melanoma, choriocarcinoma)
Treated metastatic disease (e.g., radiofrequency ablation)

1-3 Signal Loss in Liver on Chemical Shift Imaging

Hepatocellular (Common)

Diffuse steatosis
Focal steatosis
Lipid containing hepatocellular neoplasms
  Common: hepatic adenoma
  Uncommon: well-differentiated hepatocellular carcinoma
  Rare: follicular nodular hyperplasia

Nonhepatocellular (Rare)

Hepatic angiomyolipoma
Metastatic germ cell tumor
Hepatic lipoma

T2-Weighted Imaging (WI)

The T2-relaxation time of liver is shorter than for most other abdominal tissues, including spleen.[3] Nonsolid liver lesions have long T2-relaxation times and are easily detected on T2-WIs. Solid masses such as hepatocellular carcinoma and hepatic metastases have shorter T2-relaxation times compared with nonsolid lesions and may be relatively inconspicuous on T2-WIs.

Multishot or single-shot echo-train pulse sequences have replaced conventional spin-echo techniques for T2-WI of the liver (as well as for evaluation of other organs in the abdomen and pelvis). These pulse sequences utilize one or more excitation pulses followed by two or more 180° refocusing pulses, the echo train. Each of the multiple spin echoes within an echo-train sequence is acquired with a different amplitude phase-encoding gradient, and

therefore the resulting image contains data with different TE values. The effective TE refers to the TE at which the lowest amplitude phase-encoding gradients are applied. Low amplitude phase-encoding gradients provide the high-contrast, low-resolution data of central k-space, whereas high amplitude phase-encoding gradients provide the high-resolution, low-contrast data of peripheral k-space.

Echo-train T2-W pulse sequences can be performed without or with breath-holding techniques. Non–breath hold echo-train T2-W pulse sequences benefit from use of fat suppression and respiratory triggering.[4,5] Respiratory triggering requires a pneumatic bellows that is wrapped around the patient's torso. As only a portion of the respiratory cycle is used for data acquisition, respiratory triggering necessitates a long TR and is therefore easily adapted to multishot echo-train T2-W pulse sequences. Single-shot echo-train T2-weighted pulse sequences incorporate half-Fourier reconstruction (interpolation of k-space data) to reduce acquisition time. The subsecond acquisition time of single-shot T2-W sequences is useful with patients unable to comply with breath holding or for whom rapid scanning is required.[3] In comparison with multishot echo-train T2-W sequences, single-shot techniques produce images with decreased signal-to-noise ratios and increased blurring and consequently are less sensitive in the detection of smaller or low-contrast lesions.[3] T2-W sequences utilizing a TE of at least 160 ms allow improved discrimination between nonsolid hepatic lesions, such as cysts and hemangiomas, and solid lesions.[6,7] A T2-W sequence with an even longer TE (e.g., 600-700 ms) can discriminate between a hepatic cyst and hemangioma based on the higher persistent SI of the former.[8] Heavily T2-W sequences are also used for magnetic resonance cholangiopancreatography (MRCP; see Chapter 2).

Short Tau Inversion Recovery Imaging

Short tau inversion recovery (STIR) pulse sequences provide fat-suppressed images with additive T1-weighted and T2-weighted contrast. STIR pulse sequences incorporate a preparatory 180° inversion pulse prior to the excitation pulse. The interval between the inversion pulse and excitation pulse is referred to as the inversion time (TI). At a TI of 150 to 170 ms at 1.5 T, the SI of fat is null. Similar to T2-WIs, fluid and most pathologic tissues will appear hyperintense on STIR images. The echo-train technique can be incorporated into the STIR pulse sequence to shorten the acquisition time.

T2 Star (T2*)-Weighted Imaging

GRE T2*-weighted pulse sequences are used for optimal detection of hepatic iron deposition. GRE sequences lack the 180° refocusing pulses of SE or echo-train sequences and therefore do not correct for phase shifts incurred by magnetic field inhomogeneity or static tissue susceptibility gradients. T2*-contrast reflects the effective spin-spin relaxation time resulting from true T2-decay and inhomogeneity effects. The susceptibility effect of iron results in signal loss that is most conspicuous on T2*-WIs. T2*-W GRE sequences are used after the administration of iron-containing reticuloendothelial system contrast agents. These contrast agents are cleared from plasma by the Kupffer cells present in normal hepatic parenchyma and some hepatocellular lesions. The susceptibility effect induced by the iron-containing contrast results in signal loss in the normal hepatic parenchyma and renders nonhepatocellular lesions, such as metastases, hyperintense. While MR angiography is currently performed with gadolinium-enhanced techniques, T2*-W sequences can be useful for depicting the direction of flow when specific saturation pulses are applied. This information may be useful in evaluating the portal venous system or portosystemic collateral vessels/varices.[3]

Contrast-enhanced Imaging

Four major classes of intravenously administered contrast agents are used for hepatic and abdominal MR imaging: nonspecific extracellular, hepatocyte-specific, reticuloendothelial system-specific, and blood pool-specific.[9] The nonspecific extracellular agents are chelates of gadolinium, a paramagnetic metal that shortens the T1-relaxation time of surrounding molecules. Chelation is required because of the toxicity, biodistribution, and efficacy of the free gadolinium ion.[10] The nonspecific extracellular gadolinium chelates diffuse rapidly from the intravascular space into the extracellular space, similarly to the iodinated contrast agents used in CT. While iodinated contrast agents are directly imaged by radiographic techniques, it is the paramagnetic effect of gadolinium on surrounding protons that is detected by MR.[11] Nonspecific extracellular gadolinium chelates are excreted via glomerular filtration.

Hepatocyte-specific agents are chelates of gadolinium or manganese that show variable excretion through the hepatobiliary system. Increasing the lipophilicity of the gadolinium chelate allows hepatocyte uptake. Manganese-based compounds partially dissociate in the circulation; the manganese ions are excreted by the hepatobiliary system, kidneys, pancreas, and gastric mucosa.[9] Reticuloendothelial system–specific agents are superparamagnetic iron oxide formulations cleared from the plasma by the reticuloendothelial system of the liver (80%) and spleen (12%) and subsequently eliminated in the lymph nodes and bone marrow.[9] Blood pool–specific agents include ultrasmall iron oxide particles and proteinaceous or polymeric complexes of gadolinium that remain in the bloodstream for an extended period of time.

The nonspecific extracellular gadolinium chelates are the most widely used of the MR imaging contrast agents. For optimal detection and characterization of hepatic lesions with this class of agents, dynamic imaging is often needed. Prior to administration of

gadolinium chelates, precontrast imaging is acquired to assess anatomic coverage and the patient's breath-hold capacity.[12] In addition, unenhanced images serve as a baseline for comparison to the enhanced images and can also be subtracted from contrast-enhanced images. Subtraction imaging can improve MR angiographic reconstructions and detection of enhancement in masses that are hyperintense on unenhanced T1-WIs.[12,13]

Postcontrast imaging is classified into three phases: hepatic arterial dominant, portal venous, and hepatic venous or interstitial.[9,14] The hepatic arterial-dominant phase occurs 15 to 30 seconds after rapid bolus injection of contrast agent. Images obtained during this phase show enhancement of the hepatic arteries and possibly the main portal veins. However, there is no enhancement of the hepatic veins and minimal hepatic parenchymal enhancement. The hepatic arterial-dominant phase is important in the detection of hypervascular lesions and the evaluation of the hepatic arterial system. The portal venous phase occurs 45 to 75 seconds after contrast agent administration. During this phase, the portal veins, hepatic veins and hepatic parenchyma are maximally enhanced. This phase is optimal for detection of hypovascular lesions. The hepatic venous, or interstitial, phase spans from 90 seconds to 5 minutes after injection of contrast agent. This phase is useful for characterizing lesions that show continued enhancement, such as hemangiomas, or lesions with a large extracellular space, such as intrahepatic cholangiocarcinoma.

The variable circulatory status of patients requires a reliable and reproducible method for coordinating imaging, particularly acquisition of central k-space data, with the hepatic arterial-dominant phase. Commercially available methods include timing-runs, automated bolus detection and triggering, and real-time or "fluoroscopic" bolus detection with operator triggering.[15] (See Chapter 11.) The use of a power injector standardizes injection rates,[16] optimizes MR angiography, and has proven superior to manual injection.[17,18]

Dynamic gadolinium-enhanced imaging is performed with pulse sequences that enable coverage of the entire liver within a reasonable breath-hold (less than 25 s). Three-dimensional, or volumetric, GRE T1-W sequences confer several advantages over two-dimensional pulse sequences.[12] Three-dimensional GRE T1-W sequences enable acquisition of thinner sections without intersection gaps, fat suppression, higher signal-to-noise ratios, and similar image contrast within the same breath-hold duration as two-dimensional sequences. Volumetric acquisitions provide isotropic data sets that optimize postprocessing techniques, such as multiplanar reconstructions or volume rendering.

PRIMARY HEPATIC MASSES

Benign Hepatocellular Neoplasms: Adenoma and Focal Nodular Hyperplasia

Hepatocellular Adenoma (Box 1-4)

Hepatic adenoma is a benign hepatic neoplasm occurring most commonly in women taking oral contraceptive medications. The incidence of hepatic adenomas increases with the duration of oral contraceptive medication use and the dosage of estrogen.[19,20] Anabolic-androgenic steroids used for medical indications or abused by athletes are associated with a number of hepatic diseases including hepatic adenomas.[21] Hepatic adenomas, often multiple, develop with increased incidence in patients with glycogen storage diseases types I and III.[22] Hepatic adenoma may be incidentally detected at cross-sectional studies performed for unrelated reasons, or the patient may have acute or chronic pain, a palpable mass, or abnormal liver function tests.[23,24]

Hepatic adenoma is composed of benign hepatocytes arranged in large plates or cords without an

1-4 Hepatic Adenoma

Clinical

Benign hepatocellular neoplasm
Potential for hemorrhage (common) and malignant transformation (rare)
Risk factors: oral contraceptives (most common), anabolic-androgenic steroids, and glycogen storage diseases

Pathology

Mean diameter of 5 cm, multiple in 30%
Hepatocytes, Kupffer cells (usually nonfunctioning), no bile ducts, pseudocapsule of compressed parenchyma and/or fibrosis

MRI

T1-WI: SI varies with presence of lipid, hemorrhage, and necrosis; portions of tumor isointense to hyperintense to liver
Intratumoral lipid common, confirmed by chemical shift imaging
T2-WI: SI variable but usually hyperintense to liver
Hypervascular on dynamic CE imaging, but not as vascular as FNH
No central scar

acinar architecture.[25-27] The plates of hepatocytes are separated by dilated sinusoids, which in addition to feeding arteries produce the hypervascularity of adenomas.[26,27] Adenoma cells contain glycogen and lipid.[25,27] Kupffer cells may be present in adenomas but usually are nonfunctioning, and bile ducts are absent.[25,27] A fibrous capsule or pseudocapsule composed of compressed parenchyma and/or fibrosis is usually present.[26,28]

Complications of hepatic adenomas include hemorrhage with possible rupture of the liver[27,29-31] and rare malignant transformation to hepatocellular carcinoma.[30,32,33] Hemorrhage within an adenoma is thought to be related to infarction as the tumor outgrows its blood supply.[27] A hemorrhagic adenoma may rupture through the liver, resulting in hemoperitoneum with possible shock.[34] Rupture of a hemorrhagic adenoma is related to its proximity to the liver surface and the thickness of the fibrous tumor capsule, if present.[31] The true risk of malignant transformation is uncertain but was present in 5 of 39 patients in one series.[30] Although adenomas have been shown to resolve completely after the cessation of oral contraceptive medications,[35,36] this resolution does not preclude the subsequent development of hepatocellular carcinoma.[20] Liver cell dysplasia may develop within an adenoma and is an irreversible premalignant change.[20]

Hepatic adenomas range in size from 1 to 19 cm, with a mean diameter of 3 to 5 cm.[24,37,38] The heterogeneous MR appearance of hepatic adenoma reflects the variable presence of intralesional steatosis, hemorrhage, peliosis hepatis, necrosis, fibrous encapsulation, rare central scars, and large tumoral vessels.[24,27,28,37] On T1-WIs, adenomas reveal variable SI but often have components that are hyperintense to surrounding liver parenchyma.[24,28,37] Hyperintense T1 foci can be from intracellular lipid or hemorrhage (Figs. 1-1 and 1-2).[24] Chemical shift imaging can confirm the presence of intralesional steatosis (see Fig. 1-1). On T2-WIs adenomas have variable SI but usually have some hyperintense components.[24,28,37] Hemorrhage and necrosis result in the heterogeneous T2 SI.[37] Most adenomas show hypervascularity on the arterial phase of dynamic contrast-enhanced (CE) T1-WIs.[28,37]

A pseudocapsule of compressed hepatic parenchyma or fibrosis may be identified at MR.[24,28,37] On T1-WIs, this pseudocapsule is typically hypointense to adjacent liver parenchyma.[28] The T2-W appearance of this pseudocapsule is more variable, with an approximately equal number being hyperintense, isointense, or hypointense to adjacent liver parenchyma.[28]

The main differential diagnosis for hepatic adenoma includes two other hypervascular hepatocellular lesions: focal nodular hyperplasia and hepatocellular carcinoma. Except for the central scar, focal nodular hyperplasia is typically homogeneously isointense or nearly isointense to liver parenchyma on both T1- and T2-WIs, whereas adenoma is usually of heterogeneous SI. In addition, FNH usually contains a central scar, a rare finding in hepatic adenoma.[37]

Hepatic adenomas can be indistinguishable hepatocellular carcinoma based only on the MR imaging features of the lesion, although vascular invasion does not occur in hepatic adenomas. Hepatocellular carcinoma typically develops in patients with cirrhosis whereas hepatic adenomas occur in young women who have taken oral contraceptive medications. Serum α-fetoprotein is usually elevated with hepatocellular carcinoma but not with hepatic adenomas.

The management of hepatic adenomas is somewhat controversial. Surgical resection has been advocated to eliminate the known risks of life-threatening hemorrhage and malignant transformation.[31] A more selective approach to management has also been proposed.[38] In patients with lesions less than 5 cm and normal α-fetoprotein levels, cessation of oral contraceptives, counseling regarding pregnancy, and serial imaging could be considered as an alternative to surgery.[38] Hepatic arterial embolization is preferred over surgery for the acute management of hemorrhage.[38]

Liver Adenomatosis

Hepatic adenomatosis was initially described as 10 or more hepatic adenomas occurring in an otherwise normal liver (absence of glycogen storage disease), unrelated to the use of oral contraceptive medications or anabolic-androgenic steroids, with associated abnormalities in liver function tests (serum alkaline phosphatase and gamma-glutamyl transpeptidase) occurring in either women or men.[39] Recently, liver adenomatosis was defined as greater than three adenomas.[40] The majority of lesions in hepatic adenomatosis are not estrogen dependent.[41] Two forms of liver adenomatosis have been described: multifocal and massive.[42] Management of the multifocal form can be surgical resection of the larger or more complicated lesions. Liver transplantation is reserved for the more aggressive form of the disease.[42] One group advocates close surveillance for asymptomatic patients with small lesions (≤3 cm) because of the presumed lower risk of intraperitoneal hemorrhage.[40] The MR imaging characteristics of individual adenomas in liver adenomatosis (see Fig. 1-1) are similar to the more common solitary lesions that develop in women taking oral contraceptive medications.[41]

Focal Nodular Hyperplasia (Box 1-5)

Focal nodular hyperplasia (FNH) is a benign tumor thought to represent a hyperplastic response of the hepatic parenchyma to a preexisting arterial malformation.[43] FNH is the second most common benign liver tumor after hemangioma.[44] FNH is most commonly detected in women of reproductive age but can rarely occur in men and children.[43,45] Most cases of FNH are incidentally discovered at autopsy, surgery, or imaging studies and are asymptomatic. Large lesions may be symptomatic because of distention of the liver capsule or mass effect on adjacent organs.[43] Oral contraceptive medications do not initiate development of FNH; however, the relationship

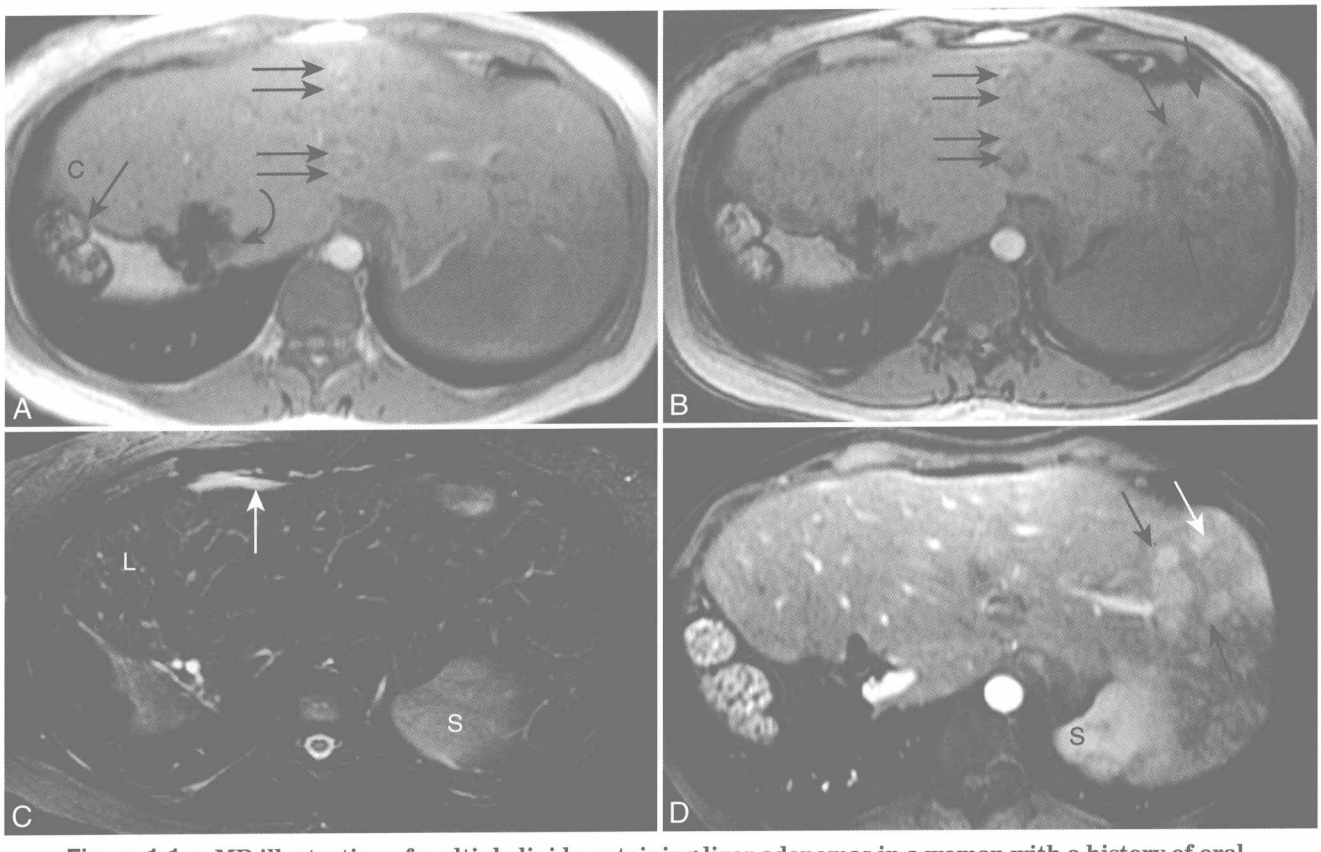

Figure 1-1 ▪ MR illustration of multiple lipid-containing liver adenomas in a woman with a history of oral contraceptive medication use; prior right lobectomy established the diagnosis of adenomatosis. A and **B**, T1-WIs show hypertrophy of the patient's remaining left lobe. No liver lesions are revealed on the in-phase image (**A**), but multiple hypointense liver lesions *(arrows)* are present on the opposed-phase image (**B**). Isointensity to liver on in-phase imaging and the presence of intracellular lipid (established by loss of SI on opposed-phase imaging) both indicate that the lesions are of hepatocellular origin. There is loss of SI on the in-phase image (with a longer TE) within right colon (*arrow* C) and adjacent to surgical clips *(curved arrow)*. Round "pseudolesions" *(double black arrows)* of variable SI are located anterior to the hyperintense aorta. The high SI within the aorta and the pseudolesions are secondary to flow-related enhancement and pulsation artifact, respectively. Applying a superior saturation band to eliminate signal from arterial blood entering the top of the imaging volume could have minimized both. **C**, Fat suppressed T2-WI does not depict the liver lesions. Note the normal difference in T2 SI between the hypointense liver (L) and hyperintense spleen (S). The high SI anterior to the liver represents unsuppressed fat *(arrow)* and should not be mischaracterized as loculated fluid. Superiorly located perihepatic fat is not suppressed secondary to localized magnetic field inhomogeneity from adjacent lung parenchyma.[491] **D**, Arterial phase CE T1-WI shows multiple hypervascular masses *(arrows)*. The heterogeneous enhancement of the spleen (S) is normal during this phase of enhancement.

between oral contraceptive medication use and growth of FNH is less clear. One study showed no relationship between oral contraceptive use and the number or size of FNH lesions,[46] whereas others showed lesion regression after discontinuation of oral contraceptive medications.[47]

FNH is solitary in 80% to 95% of patients.[43] The mass is composed of nodules of hyperplastic hepatocytes and small bile ductules surrounding a central fibrous scar.[26] The central scar contains dense connective tissue and blood vessels that may have thick, myxomatous walls.[26] Unlike neoplasms, growth of FNH is proportional to its vascular supply. Hemorrhage and necrosis are unusual, and rupture of FNH is extremely rare.[43] The mean diameter of FNH is 5 cm.[45] Malignant transformation has not been reported.

MR has greater sensitivity and specificity in the diagnosis of FNH compared with either CT or sonography.[44] FNH is typically isointense or slightly hypointense to liver parenchyma on T1-WI (Fig. 1-3; see Fig. 3-4).[43,48-50] The rare presence of lipid within FNH is usually associated with diffuse hepatic steatosis.[51] FNH is isointense to slightly hyperintense on T2-WI. A central scar can be revealed at MR in 75% to 80% of FNH lesions.[44,48,52] The central scar is characteristically hypointense to the surrounding lesion on T1-WIs and hyperintense on T2-WIs (see Figs. 1-3 and 3-4).[43,48-50] Scar hyperintensity on T2-WIs is related to the presence of blood

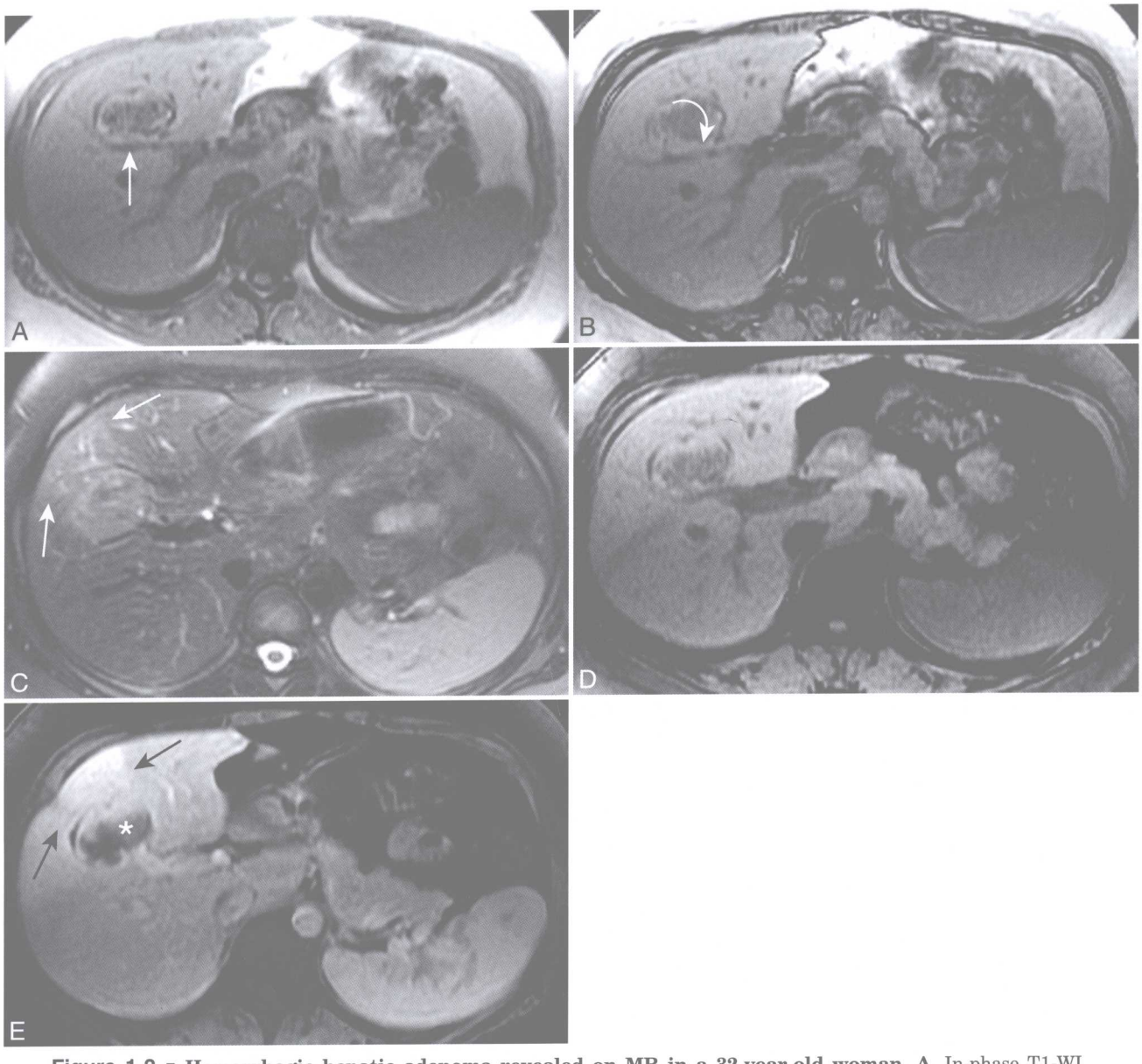

Figure 1-2 ▪ Hemorrhagic hepatic adenoma revealed on MR in a 32-year-old woman. A, In-phase T1-WI (TE = 4.2) shows a mass with a hyperintense peripheral rim *(arrow)* relative to the surrounding liver. The central portion of the mass is hypointense to liver parenchyma. **B**, Opposed-phase image (TE = 2.5) shows that the rim remains hyperintense consistent with protein or blood rather than lipid. Dependent debris is present *(curved arrow)*. **C**, Fat-suppressed T2-WI shows the mass is slightly hyperintense to liver. A wedge-shaped area of increased SI *(arrows)* peripheral to the mass likely represents edema from venous outflow obstruction. **D** and **E**, Fat suppressed T1-WIs obtained before (**D**) and after (**E**) the arterial-phase of CE show that the hemorrhagic central portion (*) of the mass does not enhance. A peripheral wedge-shaped area of increased enhancement *(arrows)* represents a transient-hepatic intensity difference, likely due to portal vein compression and compensatory increased hepatic arterial flow. It may be difficult to detect viable, enhancing portions of an adenoma that has bled. Subtraction imaging can reveal subtle enhancement within a hemorrhagic neoplasm.

vessels, bile ductules, and edema within myxomatous tissue.[43,44]

The three typical unenhanced MR imaging features of FNH—homogeneous T1 isointensity to hypointensity, homogeneous slight T2 hyperintensity, and T2 hyperintense central scar—are all present in approximately one third of lesions.[43] Atypical MR imaging findings of FNH include absence of the central scar, hypointensity of the scar on T2-WIs, nonenhancement of the scar, presence of a pseudocapsule, marked T1 or T2 lesion hyperintensity of the lesion, and heterogeneous SI.[49] Some of these atypical MR features are often present in the uncommon telangiectatic subtype of FNH.[44,53]

1-5 Focal Nodular Hyperplasia

Clinical

Benign, asymptomatic mass thought to represent hyperplastic response to preexisting arterial malformation
Most common in women of reproductive age
If a diagnosis can be established by MR, surgery can be avoided

Pathology

Hyperplastic hepatocytes, small bile ductules surrounding central fibrovascular scar, Kupffer cells present
Median diameter of 3 cm, mean diameter of 4 cm, multiple in approximately 20%

MRI

Mass

T1-WI: isointense to slightly hypointense to liver
T2-WI: isointense to slightly hyperintense to liver
Markedly hypervascular on dynamic CE imaging, isointense on portal venous phase, and slightly hyperintense on delayed phase

Central Scar

T1-WI: hypointense to surrounding mass
T2-WI: hyperintense to surrounding mass
CE imaging: hypovascular to mass on arterial phase with increased enhancement on delayed phase

On dynamic CE T1-WI, FNH shows marked arterial phase enhancement (see Fig. 1-3).[43,48,50,54] FNH becomes isointense to adjacent liver parenchyma on portal venous phase images and is slightly hyperintense on delayed images.[43,50,54] The central scar shows decreased enhancement relative to the surrounding lesion on arterial phase images[48] and almost always is hyperintense on delayed phase images (see Figs. 1-3 and 3-4).[43,48,50,52,54]

The management of asymptomatic FNH with typical MR imaging features is nonsurgical.[55,56] In contrast to hepatic adenoma, the negligible risk of hemorrhage and lack of malignant potential allow safe observation of FNH. If clinical, laboratory, or imaging data are inconsistent with a diagnosis of FNH, surgical biopsy is recommended.[56] In cases of indeterminate characterization after a gadolinium-enhanced MR examination, one could consider performing MR with a hepatocellular-specific contrast agent to confirm the hepatocellular origin of the lesion or the presence of a central scar.[44,57] Clinical history of chronic liver disease, malignancy, abnormal liver function tests, elevated serum α-fetoprotein, atypical imaging features, or increasing size should lead to biopsy for histologic confirmation. The risk of indeterminate or incorrect results with percutaneous biopsies has resulted in the use of large surgical biopsy specimens to establish a diagnosis of FNH and exclude hepatic adenoma.[55,56]

Fibrolamellar Hepatocellular Carcinoma (Box 1-6)

Fibrolamellar hepatocellular carcinoma (FL-HCC) is a rare subtype of hepatocellular carcinoma (HCC) with distinct clinical, pathologic, and imaging features. FL-HCC occurs in young patients, typically during the second or third decades, with an equal distribution between women and men.[58] As opposed to HCC, most patients who develop FL-HCC do not have a history of cirrhosis or other liver disease.[58] Clinically, patients may present with pain, hepatomegaly, palpable mass, and cachexia.[58] More than 85% of patients with FL-HCC have normal serum α-fetoprotein levels.[58]

1-6 Fibrolamellar Hepatocellular Carcinoma

Clinical

Rare; incidence of 1/million/year
M = F, present in second to third decades
Presentation may include pain, hepatomegaly, palpable mass, and cachexia
Serum α-fetoprotein usually normal (>85% of patients)

Pathology

Malignant hepatocytes separated by fibrous sheets (lamellae)
Central fibrous scar is common
Large and infiltrative, mean diameter of 13 cm

MRI

Mass

T1-WI: homogeneously hypointense to liver
T2-WI: heterogeneously hyperintense to liver
Dynamic gadolinium-enhanced: heterogeneous enhancement on arterial and portal venous phases
Aggressive lesions: possible portal vein invasion and/or extrahepatic extension

Central Scar

T1-WI: hypointense to mass and liver
T2-WI: hypointense to mass and liver
Scar usually does not enhance